applied sciences

MDPI

Review

Common Organizational Principles of Active Sensing in Rat Mystacial Touch and Human Vision

Sebastian Haidarliu [1], Guy Nelinger [2], Ehud Ahissar [1,*] and Inbar Saraf-Sinik [1]

[1] Department of Brain Sciences, The Weizmann Institute of Science, Rehovot 7610001, Israel; sebastian.haidarliu@weizmann.ac.il (S.H.); inbar.saraf-sinik@weizmann.ac.il (I.S.-S.)
[2] Department of Biological and Experimental Psychology, Queen Mary University of London, London E1 4NS, UK; g.nelinger@qmul.ac.uk
* Correspondence: ehud.ahissar@weizmann.ac.il

Abstract

Each mammalian species has sensory systems adapted to the demands of its ecological environment. Here, we compare two highly divergent active sensing systems: mystacial tactile sensing in nocturnal rats, which uses whisker movements to explore nearby objects, and human vision, in which eye movements redirect gaze. Although fundamentally different in their physical signals, receptors, anatomy, and sensorimotor mechanisms, both face recurring functional requirements for active sensory acquisition. We examine how these requirements are implemented across peripheral organization, sensorimotor kinematics, the physical transformation of environmental signals before receptor transduction, and sensory coding within closed sensorimotor loops. In both, spatially organized sensory arrays are maintained during active repositioning; rapid movements redirect sampling toward regions of interest, followed by finer-scale active sampling. Mechanical or optical properties of the peripheral apparatus transform environmental signals before receptor transduction, after which modality-specific neural circuits further shape sensory activity. Sensor movement structures sensory input so that multiple environmental properties can become simultaneously coded in neural activity, each potentially influencing subsequent movement components. These correspondences suggest that recurring constraints imposed by active sensing can be associated with analogous functional organization across fundamentally different sensory systems, without implying anatomical or mechanistic equivalence, convergent evolution, or a common computational algorithm.

Keywords: sensory organs; active sensing; closed-loop perception; sensory coding; whisker system; vision; peripheral biomechanics

Check for updates

Academic Editor: Thomas Lindner

Received: 3 September 2026
Revised: 26 October 2026
Accepted: 26 October 2026
Published: 29 October 2026

Copyright: © 2026 by the authors. Licensee MDPI, Basel, Switzerland. This article is an open access article distributed under the terms and conditions of the Creative Commons Attribution (CC BY) license.

1. Introduction

During evolution, mammals have developed sensory specializations adapted to the demands of their specific habitats, or Umwelts [1]. These specializations allow different species to acquire behaviorally relevant information through different sensory modalities. The ability to scan the environment and detect objects is reflected in specialized anatomical structures in the sensory organs that capture and transform physical signals of various kinds into neuronal signals [2–4]. Two examples are mystacial tactile sensing in rats, which live in low-light nocturnal conditions and rely heavily on nearby objects, and vision in humans, which predominantly provides information about more distant objects. Rats actively explore their environment by moving their whiskers through rotation and translation of follicle bases, while humans actively redirect gaze through movements of their eyes. Although

the stimuli, receptors, and mechanisms of transduction differ fundamentally, both systems support the detection, localization, and characterization of environmental objects. We use these systems as contrasting examples to ask whether common functional requirements of active sensing are associated with analogous organization across sensory modalities, without implying that the comparison isolates effects of sensory modality from species-specific anatomy, behavior, or ecology.

Despite their different modalities and evolutionary histories, both are active sensing systems and therefore face common functional requirements [5,6]. Spatially organized sensory arrays must remain stable while the sensors are actively repositioned; movements must support both rapid exploration and fine-scale sampling; interactions between the sensor and environment must be transformed into informative receptor signals; and sensory acquisition must remain coordinated with ongoing motor control. We therefore examine whether these shared constraints are associated with corresponding principles of anatomical and functional organization in the rat mystacial and human visual systems, despite their markedly different sensory substrates. To this end, we examine (1) corresponding principles of peripheral anatomical organization; (2) kinematic strategies for active sampling; (3) how peripheral physical transformations shape sensory signals before receptor transduction; and (4) how sensor movement contributes to sensory coding within closed-loop sensorimotor control.

This is a narrative, hypothesis-driven review based on representative primary studies and reviews relevant to the anatomical, biomechanical, kinematic, signal-transformation, and sensory-coding domains considered here.

2. Shared Organizational Principles in the Peripheral Apparatus

The rat follicle/whisker assembly (FWA) and the human eye differ fundamentally in the physical signals they detect and in their receptor types, yet active sensing imposes common functional requirements on their peripheral organization. In both systems, spatially organized receptors must remain mechanically stable while the sensory organ is repeatedly repositioned relative to the environment. This requires coordination between sensory and motor innervation, dedicated motor plants, and supporting structures that provide both stability and controlled mobility. Table 1 and Figure 1 compare how the rat mystacial and human visual systems implement shared functional requirements of active sensing. The pairings in Table 1 are therefore made between functional requirements and their implementations, rather than between structures at equivalent anatomical levels or scales. The paired anatomical features are not intended to imply anatomical or developmental equivalence; rather, they represent distinct implementations of analogous functional requirements.

Table 1. Functional organization of the rat mystacial and human visual systems supporting active sensing.

Functional Requirement	Functional Implementation	Rat Mystacial System	Human Visual System
Maintain spatially organized sensory sampling	Receptor spatial organization	Radially organized mechanoreceptor populations within follicles; ordered follicular array	Spatially organized photoreceptor mosaic within the retina
Maintain receptor geometry during repeated sensor movement	Structural stabilization	Tough follicular collagenous capsule with elastic proximal end	Mechanically robust collagenous sclera
Transmit sensory signals to the brain	Sensory innervation	Infraorbital branch of trigeminal (V) nerve	Optic (II) nerve

Table 1. *Cont.*

Functional Requirement	Functional Implementation	Rat Mystacial System	Human Visual System
Transmit motor commands to the sensory apparatus	Motor innervation	Facial (VII) nerve	Oculomotor (III), trochlear (IV), abducens (VI) nerves
Active repositioning of the sensory apparatus	Motor plant	Intrinsic and extrinsic whisker-pad muscles; elastic fascial structures	Extraocular muscles; elastic fibromuscular pulley
Control sensor orientation across multiple axes	Multiaxial movement	Azimuth, elevation, torsion	Horizontal, vertical, torsional rotation
Stabilize and guide the moving sensory apparatus	Mechanical support	Subcapsular fibrous mat; fascial collagenous skeleton	Orbital fascia; entheses; fibromuscular pulley
Permit repeated movement while accommodating tissue deformation	Compliance and elastic recovery	Elastic segment; flexible proximal follicle; elastic fascial structures	Tenon's capsule; elastic fibromuscular pulley; orbital soft tissues
Accommodate movement of associated neural structures	Neural/tissue accommodation	Compliant proximal follicular and surrounding tissues	Intraorbital optic nerve; retrobulbar tissues

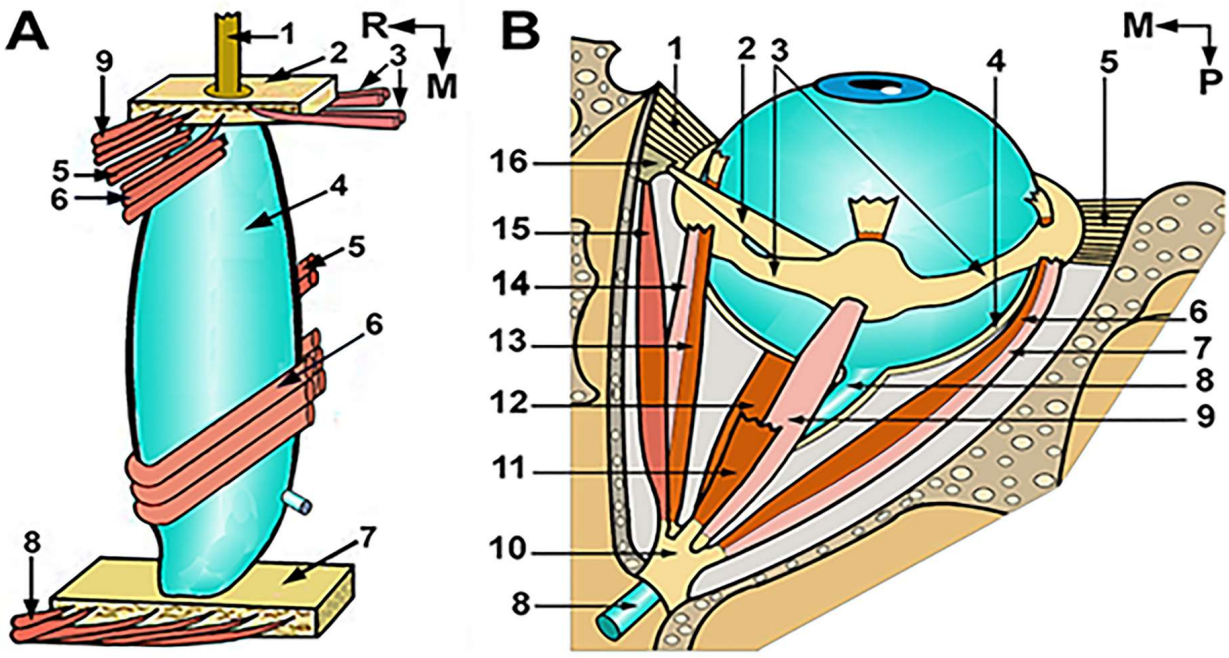


Figure 1. Schematic depiction of selected anatomical components of the rat mystacial (**A**) and human visual (**B**) apparatuses. (**A**) (1) Whisker shaft; (2) corium; (3) nasolabialis and maxillolabialis muscles; (4) follicle; (5 and 6) oblique and follicular intrinsic muscles, respectively; (7) subcapsular fibrous mat; (8) maxillary parts of the nasolabialis profundus muscle; (9) medial parts of the nasolabialis profundus muscle. (**B**) (1) Medial enthesis; (2) tendon of superior oblique muscle (SO); (3) pulley; (4) fascial membrane (Tenon capsule); (5) lateral enthesis; (6) global layer of lateral rectus muscle (LR); (7) orbital layer of LR; (8) optic nerve; (9) orbital layer of superior rectus muscle; (10) annulus Zinn; (11) levator palpebrae superioris muscle; (12) global layer of inferior rectus muscle; (13) global layer of medial rectus muscle (MR); (14) orbital layer of MR; (15) SO; (16) trochlea. M, medial; P, posterior; R, rostral.

In both systems, sensory receptors are embedded within spatially organized peripheral arrays. In the mystacial system, mechanoreceptor populations occupy stereotyped locations within individual follicle-sinus complexes, while the follicles themselves form an ordered array across the mystacial pad. In the eye, photoreceptors are organized into a spatially structured mosaic across the retina. These organizations occur at different anatomical scales

and therefore do not directly constitute equivalent receptor arrays. Rather, in both systems, spatial organization supports systematic sensory sampling as the sensory apparatus is actively repositioned.

The comparison therefore concerns how each architecture supports active sensing, rather than equivalence of the anatomical scales at which its components are organized. At the level of gross morphology, for example, the follicle is an elongated, spindle-shaped multilayered structure that has been approximated by ellipsoidal geometry in biomechanical models [7,8], whereas the eyeball is a near-spherical spheroid, varying in shape from prolate to oblate, as confirmed by in vivo measurements [9,10]. While different in geometry, both combine mechanically stable sensory structures with the capacity for controlled reorientation. The follicle is enclosed by a collagenous capsule, with a thinner and more flexible proximal region [11], whereas the sclera forms the mechanically robust collagen sheath of the eyeball. These structures differ in developmental origin and primary biological function. Their correspondence here refers to their contribution to mechanical stabilization rather than to anatomical or developmental equivalence. In both systems, these supporting structures maintain sensory-organ geometry while the surrounding motor and fascial systems enable controlled movements.

Active repositioning of the whiskers is generated by the muscular system of the whisker pad (WP) and mechanically constrained by its fascial structures (Figure 1A). Contraction of intrinsic and extrinsic muscles of the WP changes follicle and whisker orientations. During movement, whiskers can touch surrounding objects, generating and transmitting mechanical signals to the follicle, where tiny deformations activate mechanoreceptors [12]. Fascial structures maintain the structural integrity of the WP, constrain follicle orientation, transmit forces during whisking, accumulate and release elastic energy, and provide stable attachment of the WP to the skull via the subcapsular fibrous mat [13]. Importantly, this mechanical architecture combines rigidity with localized compliance: the proximal follicular region and internal whisker shaft contain flexible elements capable of reversible deformation during whisker movement, allowing controlled displacement while restoring whisker geometry across cycles [11].

The human eye similarly combines muscular control with mechanical support (Figure 1B). Six extraocular muscles actively reorient the eyeball, while orbital fascial structures stabilize and mechanically guide its movements. The sclera maintains globe geometry and protects the eyeball from mechanical deformation, while its interfaces with extraocular muscles and surrounding fascial structures contribute to force transmission and mechanical support. Together with Tenon's capsule (fascia bulbi), orbital fascia, and the fibromuscular pulley system, these structures allow rapid eye movements while constraining the globe position within the orbit [14–16].

Movement of the globe is also accommodated by the 25–30 mm intraorbital segment of the optic nerve, whose S-shaped course provides sufficient slack for eye rotation without excessive nerve stretch [17]. Retrobulbar adipose tissue separates the nerve from the extraocular muscles and further accommodates globe movement.

Thus, the anatomical correspondence between the mystacial and visual systems is most informative when considered in relation to the functional demands of active sensing. Both systems combine a spatially organized sensory apparatus with dedicated motor innervation and motor plants, while mechanically robust and compliant supporting structures preserve sensory geometry, guide movement, and accommodate repeated repositioning. These correspondences suggest that active exploration imposes common organizational constraints on otherwise fundamentally different sensory organs. We next examine how these anatomically supported capabilities are expressed in the movement strategies used for active sensing.

3. Shared Kinematic Strategies for Active Sampling

Active whisker movements are generated by the movement of the follicles, driven primarily by the follicular intrinsic muscles of the WP [18]. Fast rhythmic whisker movements (whisking) support spatial exploration of the environment and object detection. Whisking consists of alternating active whisker protraction, generated by muscle activity [19–21], and rapid retraction driven predominantly by elastic recoil following muscular relaxation [22]. Whisking can be adapted to specific behavioral needs, supporting exploratory movements that obtain sensory information, primarily about the existence, location, and coarse features of nearby objects [23,24].

Whisker kinematics in 3D can be characterized by three rotational components (azimuth, elevation, and torsion) and horizontal and vertical translational components that refer to movements of the follicle bases/mystacial array relative to the head [22,24]. Eye movements support active exploration primarily through reorientation of the eyeball with three rotational degrees of freedom, corresponding to horizontal, vertical, and torsional rotations [25]. The two systems therefore share multiaxial control of sensor orientation, but their kinematic spaces are not equivalent: mystacial movements additionally involve translation of the whisker array, whereas ocular orientation is constrained by the biomechanics of the orbit, including Listing's law and the pulley system [25]. Small translational movements of the eyeball have also been reported [26] but are not treated here as a counterpart to the translational components of mystacial motion. Tables 2 and 3 compare the organization and functional effects of the muscles controlling whisker and eye movements.

Table 2. Anatomical organization of motor systems controlling whisker and eye movements.

Muscle Features	Whisker Pad Muscles	Human Extraocular Muscles
Embryonic origin	Facial/branchiomeric muscle progenitors [27–29]	Prechordal and paraxial mesoderm [30]
Muscle type	Fast, striated, mainly type 2B [31]	Fast-contracting, specialized [30]
Muscle origin	Extrinsic, the skull; intrinsic, follicular collagenous capsule	The skull (orbit) and the fibrous collagenous ring (Annulus of Zinn)
Muscle insertion	Extrinsic, into the fascia of whisker pad; intrinsic, into follicular capsule	Into the sclera and fascia-built pulley
Fatigue resistance	Fatigue-resistant [31]	Highly fatigue-resistant [32]
Spindles	Conventional muscle spindles generally absent; whisker self-motion is signaled through alternative mechanosensory pathways [13,33,34]	Spindles of low proprioceptive capacity [35]

Both motor systems have been formalized as biomechanical control plants, in which motor commands are transformed into sensor movement through the geometry and mechanical properties of the peripheral apparatus. Numerical models of vibrissal biomechanics capture how whisker and follicular structure constrain this transformation [36], while classical and subsequent models of the oculomotor plant relate neural commands to eye movements through the dynamics of the extraocular muscles, globe, and orbital tissues [15,37]. These models provide a formal basis for treating both systems as sensorimotor plants, without implying equivalent mechanics or control laws.

The motor plants that move the FWAs and eyes support movements operating at different spatial and temporal scales. In both systems, sensor movements are coordinated with head and body movements to redirect sampling toward a region of interest, although the relative contributions of sensor, head, and body movements differ between modalities [38–41]. These coordinated movements extend the spatial range over which the sensory

apparatus can be positioned, while finer sensor movements regulate sampling within the selected region. Rapid, large-scale movements such as whisker protraction and saccades first reposition the sensory apparatus toward a region of interest, followed by slower, finer movements that support detailed sampling of that region [39,40,42,43].

Table 3. Functional effects of the mystacial pad and extraocular muscle activity on sensor movement.

Movement Component	Rat Whisker Pad		Human Eye	
	Muscles	**Whisker and Follicle Movement**	**Muscles**	**Eyeball Movement**
Horizontal (azimuth)	Follicular intrinsic; medial parts of the nasolabialis profundus	Protraction; rostral translation	Rectus lateralis	Abduction
	Maxillolabialis and Nasolabialis	Retraction	Rectus medialis	Adduction
Torsional (axial rotations)	Oblique intrinsic	Clockwise and counterclockwise torsion	Superior and inferior oblique	Intorsion and extorsion
Vertical (elevation)	Nasal transversal	Elevation	Superior rectus	Elevation
	Buccinator of the orbicularis oris	Downward deflection	Inferior rectus	Depression

Saccades and whisker protraction differ in their kinematics and in their coupling to sensory acquisition. During a saccade, rapid sensor relocation is comparatively segregated from detailed visual acquisition, although visual and internal feedback signals contribute to the broader control of gaze across and between saccades [38,44]. In contrast, during whisker protraction, sensory acquisition and sensor movement can remain tightly coupled at within-cycle timescales. Although whisker protraction begins with rapid acceleration, its velocity decreases later in the movement, and contact with objects can further modify the ongoing trajectory via rapid sensory feedback. Touch-induced pumps, for example, occur within the same whisking cycle, prolong contact, and enable continued palpation within a restricted spatial range [45–47].

Thus, both systems organize active sensing as a sequence in which rapid sensor relocation is followed by finer-scale active sampling, while the sensorimotor coupling underlying these movements differs substantially between modalities. The systems therefore share a closed-loop organization of active exploration, but not equivalent feedback delays or cycle-by-cycle control. Illustrative movement characteristics reported for the two systems are summarized in Table 4. The comparison distinguishes movement scale, sensor orientation, translational motion, and movement dynamics because these dimensions are not directly equivalent across the two systems.

Table 4. Types and parameters of movements in sensory organs of the rat mystacial tactile and human visual systems.

Motion Characteristics	Rat Mystacial Tactile System	Human Visual System
Large-scale sensor repositioning	Whisking, large whiskers, amplitude 70–108° [48,49], coarse spatial resolution	Saccades, amplitude up to ~90° [50]; coarse spatial resolution

Table 4. *Cont.*

Motion Characteristics	Rat Mystacial Tactile System	Human Visual System
Fine-scale sensory sampling	Head/snout movements during close exploration [42,51]; whisker velocities associated with head movements are on the order of 4 cm/s [52]; local whisker and microvibrissae movements [22,23]	Ocular drifts, on the order of 1°/s [53–55]
Rotational components	Azimuth, elevation, torsion [22,24]	Horizontal, vertical, torsional [25]
Torsional excursion	32° [56]	8° [57]
Translational components	Horizontal and vertical components of mystacial movement [22,24]	Small translational movements of the eyeball [26]
Peak horizontal angular velocity	~500–1000°/s [48,49]	450°/s [58,59]; 700°/s [60–62]
Horizontal angular acceleration	~20,000°/s^2 [48,49]	12,000–30,000°/s^2 [63,64]
Torsional angular velocity	200°/s [56]	100°/s [57]
Effective movement pivot *	Distal follicle end, with a movement-dependent shift along the follicle axis [22,24]	Pivot/center of rotation within the eyeball [65]; the eyeball also undergoes small translational displacements during gaze [26]

* The whisker pivot refers to an effective rotation point within the follicle, which may shift with movement, whereas the ocular pivot refers to the effective center of rotation of the eyeball within the orbit. These are system-specific kinematic constructs rather than anatomically equivalent structures.

At finer spatial scales, local snout and whisker movements support tactile sampling through the rhinarium and microvibrissae [66–68], whereas ocular drift continuously shifts the retinal image across neighboring photoreceptors [38,69]. Thus, although the specific kinematics and sensory consequences of these movements differ, both systems combine large-scale sensor repositioning with finer-scale movements that sustain local sensory acquisition.

Thus, despite differences in their kinematics and temporal coupling to sensory feedback, both systems organize active exploration across complementary movement scales, combining rapid sensor repositioning with finer-scale sampling of regions of interest.

4. Peripheral Processing Further Shapes Sensory Signals

In both systems, sensory acquisition involves a sequence of transformations that begin before receptor transduction and continue within neural circuits. At the pre-receptor stage, the physical properties of the peripheral apparatus reshape the environmental signal: whisker and follicular biomechanics transform mechanical interactions in the mystacial system, whereas the optical apparatus transforms incoming light in vision. Resulting sensory signals undergo further modality-specific neural processing through trigeminal pathways in the whisker system and retinal circuitry in vision. The two systems therefore differ markedly in the physical nature, anatomical location, and circuitry of these transformations, while sharing the broader organization in which sensory signals are progressively structured before reaching higher-order brain areas.

During active exploration, whisker–object contact generates forces and moments at the point of contact that depend on the interaction between the whisker and the contacted surface [70]. The whisker's conical taper and intrinsic curvature shape these mechanical signals as they propagate along the shaft toward the follicle [71–73], such that the mechanical input available to the receptors differs from the original interaction. Contact-induced vibrations also propagate rapidly toward the follicle and exhibit relatively low damping [74]. The biomechanical properties of the whisker, including its resonant properties, shape these vibrations and their

temporal structure. Such temporal signatures can carry information about object location and texture. Location-related responses have been linked to selective contact sensitivity of follicle receptors [12,47,75,76]. Texture-related responses have been linked to resonant properties of the whisker [77,78] and kinetic features of frictional interactions, including slip–stick events and whisker velocity [79–81]. Resonance has been demonstrated in isolated whiskers and in awake animals and can shape the frequency-selective neural representation of vibrissal input [74,77,78]. Mechanical forces generated during whisker contact are shown in Figure 2A.

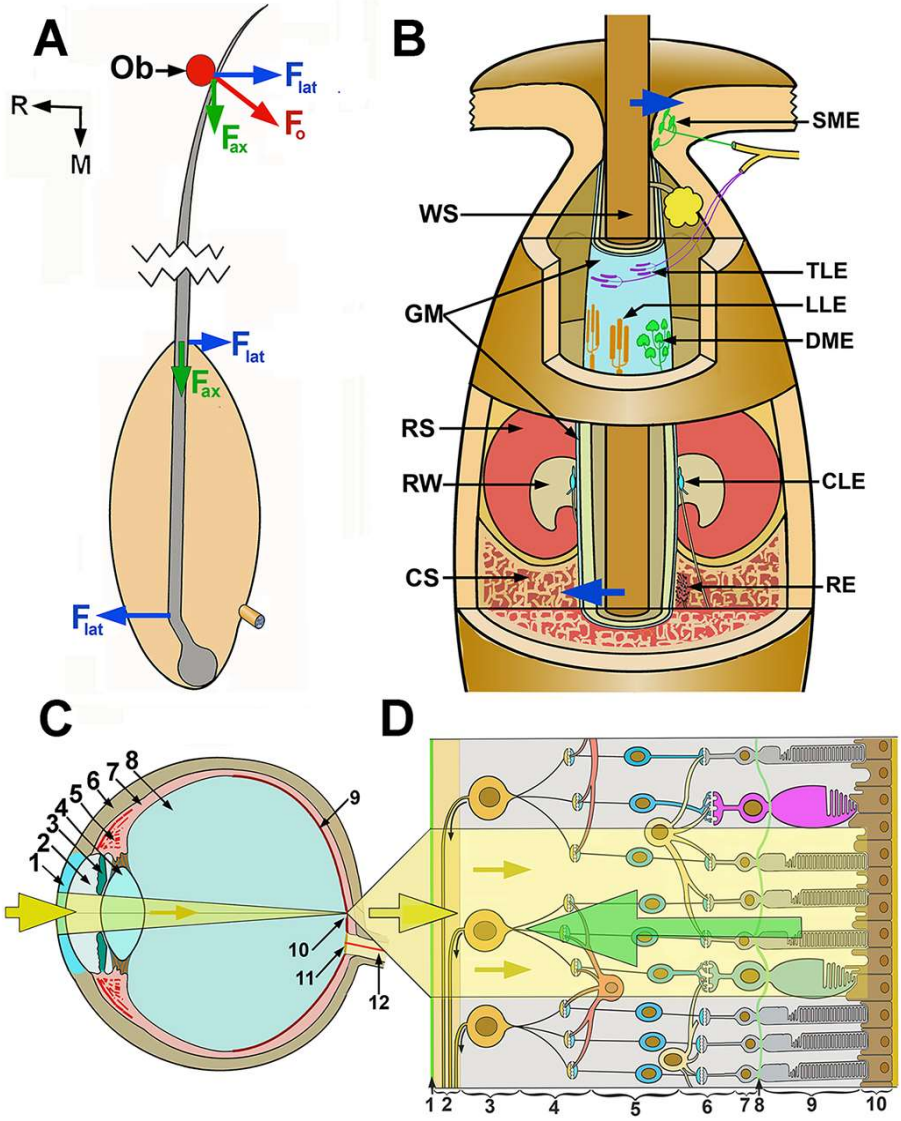


Figure 2. Peripheral transformations of sensory signals in the rat mystacial and human visual systems. (**A**) Mechanical forces and moments generated at whisker–object contact. Fax, axial force; Flat, lateral force; Fo, force exerted by the object; M, medial; Ob, object; R, rostral. (**B**) Mechanical transformation within the follicle and arrangement of mechanoreceptors. CLE, club-like endings; CS, cavernous sinus; DME, deep Merkel endings; GM, glassy membrane; LLE, longitudinal lanceolate endings; RE, reticular endings; RS, ring sinus; RW, ringwulst; SME, superficial Merkel endings; TLE, transverse lanceolate endings; WS, whisker shaft. (**C**) Optical transformation of incoming light by the cornea, iris, lens, and ocular media. (1) cornea; (2) anterior chamber; (3) iris; (4) lens; (5) ciliary muscle; (6) sclera; (7) choroid; (8) vitreous humor; (9) retina; (10) fovea; (11) blind spot; (12) optic nerve. (**D**) Retinal phototransduction and neural processing through the retinal circuit. (1) inner limiting membrane; (2) nerve fiber layer; (3) ganglion cell layer; (4) inner plexiform layer; (5) inner nuclear layer; (6) outer plexiform layer; (7) outer nuclear layer; (8) external limiting membrane; (9) photoreceptor layer; (10) retinal pigment epithelium.

Mechanical transformation continues within the follicle. The internal whisker shaft comprises a relatively rigid distal portion and a compliant elastic segment (ES) near its proximal end [11]. Forces acting on the whisker can produce localized, reversible bending and torsion of the ES, changing the position and orientation of the rigid internal shaft relative to the circumferentially organized mechanoreceptors [82–84]. Together with stabilization of the follicle base by the subcapsular fibrous mat, this mechanical organization may transform whisker motion into spatially and temporally structured patterns of mechanoreceptor activation [11].

Changes in shape or position of the internal part of the whisker shaft exert pressure on adjacent follicular structures, activating mechanosensitive ion channels in the membranes of mechanoreceptors associated with myelinated axons [85,86]. Opening of these channels generates a receptor potential that triggers action potentials (nerve impulses) in afferent nerve fibers belonging to primary sensory neurons whose cell bodies are in the trigeminal ganglion. Figure 2B shows the location of mechanoreceptors associated with myelinated axons using the symbolic shapes and colors conventionally used to represent these receptor types [8,12,87].

The distal half of the internal portion of the whisker shaft is rigid and contains a fulcrum [70,71]. Mechanoreceptors surrounding the whisker shaft are sensitive to small deformations and use Piezo2-dependent mechanotransduction mechanisms [85,86]. Experiments on mechanosensitive cells have demonstrated responses to displacements of approximately 10–13 nm [88–90]. Thus, mechanoreceptors do not transduce the external mechanical interaction directly; they transduce its mechanically transformed consequences within the follicle.

A further consequence of follicular organization is differential sensitivity to self-generated whisking and external contact. Primary afferents can distinguish these signals [47], a distinction crucial for identifying and localizing external objects [76]. A recent study combining meticulous anatomical analysis with electrically induced whisking identified club-shaped endings as mechanoreceptors that respond selectively to touch while remaining insensitive to whisking. This selectivity was attributed to their position and mechanical coupling within the follicle, including accurate positioning near the fulcrum, attachment to the shaft, specialized Schwann cells and collagen organization, and a counterweight-like mechanical arrangement [12]. These findings illustrate how peripheral morphology can selectively shape the sensory signals available for transduction.

In the visual system, incoming light is shaped by the relative motion between the eye and the environment, along with morphological adaptations of the eye. The ocular optical apparatus transforms incoming light before it reaches the photoreceptors (Figure 2C). The cornea and lens determine the spatial distribution of light at the retinal plane [9], while the iris regulates the amount of light entering the eye. The ocular media also selectively absorb and transmit different wavelengths [91,92]. These optical properties therefore shape the intensity, spatial structure, and spectral composition of the stimulus available to photoreceptors.

Upon entering the retina, photons are absorbed by rods and cones (Figure 2D), producing graded changes in photoreceptor membrane potential via a multi-step biochemical cascade [93]. The resulting signals are then transformed within the retina through interconnected bipolar, horizontal, and amacrine cell circuits [94,95] before retinal ganglion cells integrate them and generate action potentials that constitute the retina's spiking output, transmitted via the optic nerve [95]. In the mystacial tactile system, information is transmitted from mechanoreceptors via trigeminal ganglion neurons to the principal and spinal trigeminal nuclei in the brainstem [34].

Despite their different circuitry and signals, early visual and mystacial pathways exhibit several recurring organizational motifs, including topographic organization and parallel processing. One such feature is topographic organization: the spatial arrangement of retinal input is preserved in orderly visual-field representations within downstream visual struc-

tures, including the lateral geniculate nucleus, superior colliculus, and visual cortex [96,97]. Similarly, whisker-related subdivisions of the trigeminal brainstem nuclei preserve aspects of the spatial organization of the mystacial array [98]. Within individual follicles, the spatial organization of mechanoreceptors provides an additional anatomical basis for differentiated mechanosensory signaling [84,99]. Another similarity is the organization and transmission of information in parallel streams. Both systems employ several classes of receptors tuned to various stimulus parameters: vision uses rods and three cone classes with distinct spectral sensitivities [100], whereas the mystacial follicle contains multiple mechanoreceptor classes with distinct anatomical and functional properties [12,84].

The retina further segregates visual information into parallel ON and OFF pathways, signaling luminance increments and decrements, respectively, and into functionally specialized channels that contribute to the parvocellular, magnocellular, and koniocellular pathways [101]. Analogously, the rat whisker system generates ON- and OFF-like signals associated with contact onset and offset, respectively [47], and segregates active-touch information into functionally specialized lemniscal, extralemniscal, and paralemniscal pathways that differentially convey combinations of touch and whisking signals [102,103].

Lateral inhibitory interactions provide another functional parallel. In the retina, lateral interactions mediated by horizontal and amacrine cells contribute to contrast enhancement and spatial selectivity, enhancing visual borders and contrast [104]. In the trigeminal brainstem, local GABAergic inhibitory interneurons can suppress responses associated with neighboring whiskers, providing similar "center-surround" dynamics [105]. Thus, both pathways use lateral interactions that can sharpen spatial differences in sensory activity, although the underlying circuits and computations are distinct.

These correspondences concern selected functional features of early sensory processing rather than equivalence between retinal and trigeminal circuits, which differ in their anatomical locations, organization, and position within the respective sensory pathways. Despite these differences, both systems progressively transform sensory input through pre-receptor physical transformations and subsequent neuronal processing. Recurring organizational motifs include spatial organization, parallel processing, and lateral interactions, but these are implemented by modality-specific structures and circuits (Figure 3).

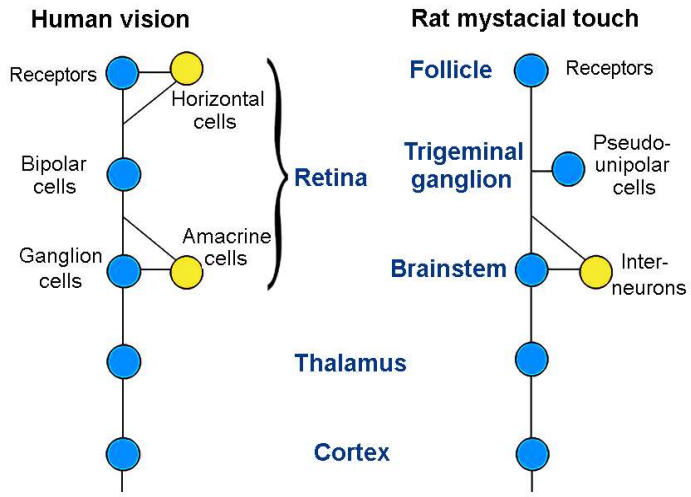


Figure 3. Schematic comparison of selected organizational features of early visual and mystacial sensory pathways. Blue circles represent excitatory cells. Yellow circles represent inhibitory cells involved in feedforward and feedback inhibition (indicated by diagonal and horizontal lines). Both systems exhibit parallel signal transmission and inhibitory interactions, although the relevant cell types, anatomical locations, and circuit implementations differ.

Importantly, in both systems, the resulting neural activity is structured in space and time by the interaction between environmental input and sensor movement [55,106]. Sensory acquisition therefore cannot be considered independently of the movements that generate and structure this activity, motivating the comparison of movement-dependent sensory coding that follows.

5. Coding and Closed-Loop Control of Sensory Acquisition

The two sensory systems also share several principles of sensory coding that emerge from active sampling. The same sampling movement can make multiple sensory variables simultaneously available in the resulting neural activity. In the whisker system, this organization has been described as "orthogonal coding", in which different properties of object location are represented through distinct aspects of the sensory activity [76,107]. Specifically, the identity of the activated sensory afferents can convey object elevation, response timing can convey azimuth, and firing rate can convey radial distance [107]. More recent population recordings further show that distinct whisker-derived variables can occupy approximately orthogonal subspaces of cortical activity [108]. More broadly, sensory variables can be represented through neuronal identity, response timing or phase, firing rate, and distributed population activity, allowing multiple properties of the sampled environment to be represented simultaneously and, in principle, read out in parallel [107,109–111]. In vision, eye movements structure the spatial and temporal sampling of the scene, producing neural activity in which multiple properties of the sampled scene can be represented through temporal, rate, spatial, and population signals [94,109,112–114]. Related principles have also been demonstrated in theoretical and synthetic studies [115,116]. Table 5 summarizes these functional dimensions and their implementations in the two systems.

Importantly, these coding dimensions arise jointly from the sensory environment and the movement of the sensory organ. Sensor trajectory determines which receptors are engaged and in what sequence, while scanning velocity transforms spatial offsets into temporal delays between receptor activations [106]. Thus, sensor motion is an integral part of the resulting sensory code, structuring the neural activity from which different stimulus variables can subsequently be read out [117].

Table 5. Functional dimensions of sensory coding during active sampling.

Coding Dimension	Rat Mystacial Tactile System	Human Visual System
Neuronal identity	Object elevation can be represented by the identity of activated sensory afferents [76,107]. Touch and self-generated whisking are differentially represented by mechanoreceptor classes, with club-like endings selectively responsive to touch [12].	Cone identity provides wavelength-selective signals through the three spectrally distinct L-, M-, and S-cone classes [100,118]. Outside the fovea, spatial position is represented by the identity/location of activated retinal neurons, whereas foveal sampling is strongly shaped by active image repositioning across the receptor mosaic [69,119].
Response timing/phase	Object azimuth can be represented by response timing relative to whisker movement [47,76,107].	The spatial structure of a briefly presented image can be represented by the relative first-spike latencies of retinal ganglion cells. Visual contrast can also be represented by response latency in V1 [109,120].

Table 5. *Cont.*

Coding Dimension	Rat Mystacial Tactile System	Human Visual System
Firing rate/ temporal structure	Radial distance can be represented by firing rate [76,107]; texture can be represented through firing rate and temporal patterns [79,80,121].	Visual contrast is represented in firing rate and temporal response structure [120]; orientation, spatial frequency, and motion direction are represented by systematic changes in neuronal firing rate in early visual cortex [122–125].
Spatiotemporal patterns	Stimulus location and complex multi-whisker patterns are represented by spatial–temporal activity across somatosensory neurons [126,127]; object shape is represented through patterns of contact across whiskers and corresponding task-specific barrel-cortex activity [128].	Spatiotemporal patterns of retinal activity represent changing visual input [94], while cortical population responses encode stimulus sequences [113]. In the human visual cortex, population receptive fields systematically represent visual-field position and spatial extent [129], providing complementary spatial and temporal dimensions for representing visual input.
Separable, simultaneous representations	Multiple object-location variables can be simultaneously represented through separable coding dimensions: afferent identity for elevation, response timing for azimuth, and firing rate for radial distance [76,107]. Distinct tactile variables also occupy approximately orthogonal subspaces of cortical population activity [108].	Multiple visual properties can be simultaneously represented through distinct coding variables, including cone identity for wavelength-selective signals, response timing for spatial structure and contrast, and firing rate for contrast, orientation, and motion [109,118,120,123,124]. Visual cortical populations can represent multiple stimulus features along approximately orthogonal dimensions, as demonstrated in nonhuman primate visual cortex [112,130].

The correspondence proposed here is functional and does not imply identical neural mechanisms. The visual coding examples include physiological evidence from nonhuman primates, where invasive population-level measurements of the corresponding neural representations are not generally available in humans.

In vision, complementary coding dimensions arise across successive levels of the visual pathway. Relative response timing can carry visual information in retinal ganglion-cell responses, while retinal circuits further transform visual signals through dynamic spatial and temporal processing [94,109].

At the cortical level, multiple visual features can be represented along distinct dimensions of population activity [112,130]. These findings provide a visual counterpart to the functional principle illustrated by the whisker system, without requiring the underlying coding mechanisms to be identical.

The same movements that structure sensory coding are themselves shaped by sensory feedback, embedding sensory acquisition within a closed sensorimotor loop. In both systems, peripheral signal processing is therefore part of the closed-loop architecture that regulates the magnitude, timing, and spatial distribution of receptor activation (Figure 4). In the whisker system, the forces generated during object contact depend on whisker position, velocity, and angle, and their resulting curvature and mechanical stresses propagate to the follicle, where they determine the magnitude and timing of mechanoreceptor activation [70,71]. This relationship is reciprocal: sensory consequences of whisker–object interaction can modify whisker movement within the same sampling cycle. Touch-induced pumps provide a particularly direct example, in which contact rapidly modifies the ongoing whisker trajectory, prolonging and refining subsequent object sampling [43,46].

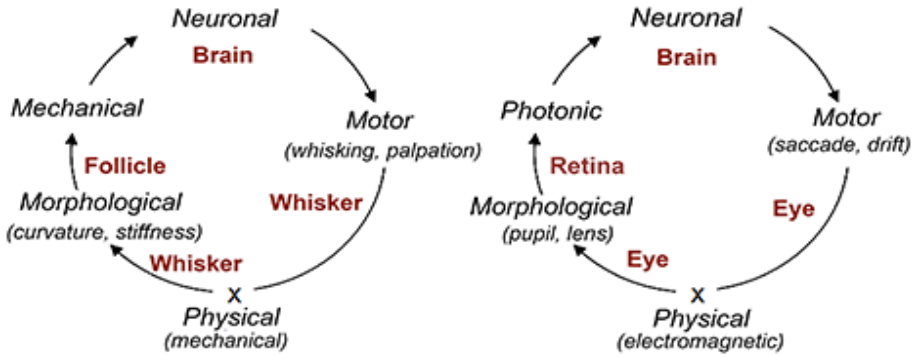


Figure 4. Loops of transformations in active sensing. Arrows indicate transformations; brown text refers to anatomical location, black text refers to processing class; X indicates interactions. Left, whisker system. Right, visual system.

In the visual system, several motor-controlled parameters regulate the input reaching photoreceptors. Pupil diameter, lens curvature, and ocular orientation are controlled by motor commands and determine the amount, focus, and spatiotemporal distribution of light reaching the retina [58,114,131]. These variables therefore shape the magnitude and timing of photoreceptor activation. In addition, fixational eye movements continuously shift the retinal image across neighboring receptors, thereby transforming spatial relationships in the visual scene into temporal relationships in retinal activity [114,115].

In both sensory modalities, the motor commands controlling these variables are continuously influenced by incoming sensory signals, forming a closed-loop architecture in which sensory input continuously guides sensor motion and configuration. Such sensorimotor loops enable organisms to actively regulate the acquisition of sensory information, for example, by selecting spatial, temporal, and spectral regions of interest, according to ongoing behavioral demands, and to converge on perceptually relevant brain-world attractors [132].

Thus, during natural behavior, in both systems, sensory coding cannot be dissociated from sensor movement. A single active sampling event can make multiple properties of the environment simultaneously available through separable dimensions of sensory activity, while the resulting neural signals provide feedback that shapes subsequent sensor movement. The sensory organ and its neural circuits therefore constitute successive components of the same closed-loop process, in which controlled movement structures the information available to neural populations and neural processing, in turn, controls how the environment is sampled.

The comparison is necessarily constrained by differences in species, sensory modality, experimental context, and the levels of neural organization represented in the literature. The proposed correspondences should therefore be interpreted as functional analogies and hypotheses about organizational principles, rather than as evidence for shared mechanisms or evolutionary convergence.

6. Conclusions

This review compares two sensory systems that evolved in different lineages, operate on fundamentally different physical signals, and support exploration of different ecological environments: the mystacial tactile system of nocturnal rats and the visual system of humans. Despite these differences, active exploration imposes common functional requirements on sensory acquisition. Both systems maintain spatially organized receptor arrays within mechanically supported sensory organs that can be actively oriented in multiple dimensions; combine rapid sensor repositioning with finer-scale movements for detailed sampling; physically transform environmental signals before receptor transduction; and

use sensor movement to structure the sensory information available to neural populations. These movement-dependent signals can make multiple properties of the environment simultaneously available through separable coding dimensions, while sensory feedback, in turn, shapes subsequent sensor movement, embedding the sensory organ itself within a closed-loop sensorimotor process.

The utility of this abstraction is also illustrated by biomimetic implementations of active sensing. Robotic whisker systems such as Whiskerbot and SCRATCHbot [133,134] incorporate whisker mechanics, active sensor movement, and tactile feedback, while a recent biomimetic robotic eye reproduced characteristic human saccade dynamics using a mechanically constrained 3D oculomotor plant and optimal control [135]. Although these engineering systems do not establish shared biological mechanisms, they demonstrate the feasibility of integrating sensor geometry, mechanical constraints, motor control, and sensory feedback within active-sensing architectures. Thus, despite their different sensory modalities and evolutionary histories, the rat mystacial and human visual systems, as active-sensing systems, face common functional requirements. The observed correspondences are consistent with the hypothesis that recurring constraints imposed by active sensing favor analogous functional solutions across otherwise fundamentally different sensory systems.

Author Contributions: S.H.: Conceptualization, Literature Review, Writing—Original Draft, Figure/Table Preparation. G.N.: Literature Review, Writing—Review & Editing, Table Preparation. E.A.: Conceptualization, Supervision, Writing—Review & Editing, Funding Acquisition. I.S.-S.: Conceptualization, Supervision, Literature Review, Writing—Review & Editing, Table Preparation. All authors have read and agreed to the published version of the manuscript.

Funding: This research was funded by the United States–Israel Binational Science Foundation (BSF, grant No. 2021327); the Weizmann–UK Collaboration; and a research grant from the Estate of Thomas Gruen.

Data Availability Statement: No new data were created or analyzed in this study. Data sharing is not applicable to this article.

Conflicts of Interest: The authors declare no conflicts of interest.

References

1. Oteiza, P.; Baldwin, M.W. Evolution of Sensory Systems. *Curr. Opin. Neurobiol.* **2021**, *71*, 52–59. [CrossRef]
2. Schlosser, G.; Musser, J.; Arendt, D. Development and Evolution of Sensory Cells and Organs. *Dev. Biol.* **2017**, *431*, 1–2. [CrossRef] [PubMed]
3. Valencia-Montoya, W.A.; Pierce, N.E.; Bellono, N.W. Evolution of Sensory Receptors. *Annu. Rev. Cell Dev. Biol.* **2024**, *40*, 353–379. [CrossRef]
4. Willemart, R.H. The Evolution of the Concept of Sensory Ecology and the Influence of Behavioral Ecology. *Anim. Sci. An. Acad. Bras. Ciênc.* **2023**, *95*, e20220302. [CrossRef] [PubMed]
5. Nelson, M.E.; MacIver, M.A. Sensory Acquisition in Active Sensing Systems. *J. Comp. Physiol. Neuroethol. Sens. Neural Behav. Physiol.* **2006**, *192*, 573–586. [CrossRef] [PubMed]
6. Yang, S.C.-H.; Wolpert, D.M.; Lengyel, M. Theoretical Perspectives on Active Sensing. *Curr. Opin. Behav. Sci.* **2018**, *11*, 100–108. [CrossRef] [PubMed]
7. Kim, J.-N.; Koh, K.-S.; Lee, E.; Park, S.-C.; Song, W.-C. The Morphology of the Rat Vibrissal Follicle-Sinus Complex Revealed by Three-Dimensional Computer-Aided Reconstruction. *Cells Tissues Organs* **2011**, *193*, 207–214. [CrossRef] [PubMed]
8. Luo, Y.; Bresee, C.S.; Rudnicki, J.W.; Hartmann, M.J.Z. Constraints on the Deformation of the Vibrissa within the Follicle. *PLoS Comput. Biol.* **2021**, *17*, e1007887. [CrossRef]
9. Navarro, R. The Optical Design of the Human Eye: A Critical Review. *J. Optom.* **2009**, *2*, 3–18. [CrossRef]
10. Verkicharla, P.K.; Mathur, A.; Mallen, E.A.H.; Pope, J.M.; Atchison, D.A. Eye Shape and Retinal Shape, and Their Relation to Peripheral Refraction. *Ophthalmic Physiol. Opt.* **2012**, *32*, 184–199. [CrossRef] [PubMed]
11. Haidarliu, S.; Nelinger, G.; Gantar, L.; Ahissar, E.; Saraf-Sinik, I. An Elastic Segment of the Whisker Shaft Enables Coding of the Whisking Phase via Whisker Torsion in Rats and Mice. *Anat. Rec. Hoboken* **2026**, *309*, 1910–1924. [CrossRef] [PubMed]

12. Muramoto, T.; Furuta, T.; Koike, T.; Bagdasarian, K.; Tonomura, S.; Takenaka, A.; Kataoka, Y.; Maeda, M.; Eguchi, A.; Kitada, M.; et al. Club-like Receptors Respond to Light Touch but Not to Whisking. *Nat. Commun.* **2025**, *16*, 11343. Erratum in *Nat. Commun.* **2026**, *17*, 1712. https://doi.org/10.1038/s41467-026-69653-0. [CrossRef]
13. Haidarliu, S.; Bagdasarian, K.; Sardonicus, S.; Ahissar, E. Interaction between Muscles and Fascia in the Mystacial Pad of Whisking Rodents. *Anat. Rec. Hoboken* **2021**, *304*, 400–412. [CrossRef] [PubMed]
14. Boote, C.; Sigal, I.A.; Grytz, R.; Hua, Y.; Nguyen, T.D.; Girard, M.J.A. Scleral Structure and Biomechanics. *Prog. Retin. Eye Res.* **2020**, *74*, 100773. [CrossRef] [PubMed]
15. Haslwanter, T. Mechanics of Eye Movements: Implications of the "Orbital Revolution". *Ann. N. Acad. Sci.* **2002**, *956*, 33–41. [CrossRef] [PubMed]
16. Stecco, C.; Hammer, W.; Vleeming, A.; De Caro, R. 4—Fasciae of the Head and Neck. In *Functional Atlas of the Human Fascial System*; Churchill Livingstone: Chatswood, NSW, Australia, 2015; pp. 103–139.
17. Salazar Corral, J.J.; Ramírez Sebastián, A.I.; de Hoz Montañana, M.R.; García Martín, E.S.; Rojas Lozano, M.D.P.; Fernández Arrabal, J.A.; López Cuenca, I.; Rojas López, M.B.; Triviño Casado, A.; Ramírez Sebastián, J.M. Anatomy of the Human Optic Nerve: Structure and Function. In *Optic Nerve*; Ferreri, F., Ed.; IntechOpen: London, UK, 2018; pp. 2–47. [CrossRef]
18. Bresee, C.S.; Luo, Y.; Alade'Fa, J.L.; Black, M.E.; Kleczka, K.J.; Bush, N.E.; Zhang, K.; Hartmann, M.J. Biomechanical Simplification of the Motor Control of Whisking. *Curr. Biol.* **2026**, *36*, 826–832. [CrossRef]
19. Carvell, G.E.; Simons, D.J.; Lichtenstein, S.H.; Bryant, P. Electromyographic Activity of Mystacial Pad Musculature during Whisking Behavior in the Rat. *Somatosens. Mot. Res.* **1991**, *8*, 159–164. [CrossRef] [PubMed]
20. Hill, D.N.; Bermejo, R.; Zeigler, H.P.; Kleinfeld, D. Biomechanics of the Vibrissa Motor Plant in Rat: Rhythmic Whisking Consists of Triphasic Neuromuscular Activity. *J. Neurosci. Off. J. Soc. Neurosci.* **2008**, *28*, 3438–3455. [CrossRef] [PubMed]
21. Wineski, L.E. Facial Morphology and Vibrissal Movement in the Golden Hamster. *J. Morphol.* **1985**, *183*, 199–217. [CrossRef] [PubMed]
22. Haidarliu, S.; Nelinger, G.; Gantar, L.; Ahissar, E.; Saraf-Sinik, I. Functional Anatomy of Mystacial Active Sensing in Rats. *Anat. Rec. Hoboken* **2024**, *307*, 442–456. [CrossRef] [PubMed]
23. Brecht, M.; Preilowski, B.; Merzenich, M.M. Functional Architecture of the Mystacial Vibrissae. *Behav. Brain Res.* **1997**, *84*, 81–97. [CrossRef] [PubMed]
24. Knutsen, P.M.; Biess, A.; Ahissar, E. Vibrissal Kinematics in 3D: Tight Coupling of Azimuth, Elevation, and Torsion across Different Whisking Modes. *Neuron* **2008**, *59*, 35–42. [CrossRef] [PubMed]
25. Klier, E.M.; Meng, H.; Angelaki, D.E. Three-Dimensional Kinematics at the Level of the Oculomotor Plant. *J. Neurosci.* **2006**, *26*, 2732–2737. [CrossRef] [PubMed]
26. Moon, Y.; Lee, J.W.; Shin, S.H.; Kim, J.N.; Lee, J.Y.; Oh, S.Y.; Lim, H.W. Positional Change of the Eyeball during Eye Movements: Evidence of Translatory Movement. *Front. Neurol.* **2020**, *11*, 556441. [CrossRef] [PubMed]
27. Trainor, P.A.; Tan, S.S.; Tam, P.P. Cranial Paraxial Mesoderm: Regionalisation of Cell Fate and Impact on Craniofacial Development in Mouse Embryos. *Development* **1994**, *120*, 2397–2408. [CrossRef] [PubMed]
28. Buckingham, M. Gene Regulatory Networks and Cell Lineages That Underlie the Formation of Skeletal Muscle. *Proc. Natl. Acad. Sci. USA* **2017**, *114*, 5830–5837. [CrossRef] [PubMed]
29. Yahya, I.; Böing, M.; Hockman, D.; Brand-Saberi, B.; Morosan-Puopolo, G. The Emergence of Embryonic Myosin Heavy Chain during Branchiomeric Muscle Development. *Life* **2022**, *12*, 785. [CrossRef] [PubMed]
30. Porter, J.D.; Baker, R.S.; Ragusa, R.J.; Brueckner, J.K. Extraocular Muscles: Basic and Clinical Aspects of Structure and Function. *Surv. Ophthalmol.* **1995**, *39*, 451–484. [CrossRef] [PubMed]
31. Jin, T.-E.; Witzemann, V.; Brecht, M. Fiber Types of the Intrinsic Whisker Muscle and Whisking Behavior. *J. Neurosci.* **2004**, *24*, 3386–3393. [CrossRef] [PubMed]
32. Fuchs, A.F.; Binder, M.D. Fatigue Resistance of Human Extraocular Muscles. *J. Neurophysiol.* **1983**, *49*, 28–34. [CrossRef] [PubMed]
33. Mameli, O.; Stanzani, S.; Mulliri, G.; Pellitteri, R.; Caria, M.A.; Russo, A.; De Riu, P. Role of the Trigeminal Mesencephalic Nucleus in Rat Whisker Pad Proprioception. *Behav. Brain Funct.* **2010**, *6*, 69. [CrossRef] [PubMed]
34. Bosman, L.W.J.; Houweling, A.R.; Owens, C.B.; Tanke, N.; Shevchouk, O.T.; Rahmati, N.; Teunissen, W.H.T.; Ju, C.; Gong, W.; Koekkoek, S.K.E.; et al. Anatomical Pathways Involved in Generating and Sensing Rhythmic Whisker Movements. *Front. Integr. Neurosci.* **2011**, *5*, 53. [CrossRef] [PubMed]
35. Ruskell, G.L. The Fine Structure of Human Extraocular Muscle Spindles and Their Potential Proprioceptive Capacity. *J. Anat.* **1989**, *167*, 199–214. [PubMed]
36. Lucianna, F.A.; Albarracín, A.L.; Vrech, S.M.; Farfán, F.D.; Felice, C.J. The Mathematical Whisker: A Review of Numerical Models of the Rat's Vibrissa Biomechanics. *J. Biomech.* **2016**, *49*, 2007–2014. [CrossRef] [PubMed]
37. Robinson, D.A. The Mechanics of Human Saccadic Eye Movement. *J. Physiol.* **1964**, *174*, 245–264. [CrossRef] [PubMed]
38. Kowler, E. Eye Movements: The Past 25 Years. *Vis. Res.* **2011**, *51*, 1457–1483. [CrossRef] [PubMed]

39. Haskins, A.J.; Mentch, J.; Botch, T.L.; Robertson, C.E. Active Vision in Immersive, 360° Real-World Environments. *Sci. Rep.* **2020**, *10*, 14304. [CrossRef] [PubMed]
40. Skyberg, R.J.; Niell, C.M. Natural Visual Behavior and Active Sensing in the Mouse. *Curr. Opin. Neurobiol.* **2024**, *86*, 102882. [CrossRef] [PubMed]
41. Stahl, J.S. Eye-Head Coordination and the Variation of Eye-Movement Accuracy with Orbital Excentricity. *Exp. Brain Res.* **2001**, *136*, 200–210. [CrossRef] [PubMed]
42. Kurnikova, A.; Moore, J.D.; Liao, S.-M.; Deschênes, M.; Kleinfeld, D. Coordination of Orofacial Motor Actions into Exploratory Behavior by Rat. *Curr. Biol. CB* **2017**, *27*, 688–696. [CrossRef] [PubMed]
43. Nelinger, G.; Saraf-Sinik, I.; Ahissar, E. Object Detection through Dynamic Motor-Sensory Convergence. *bioRxiv* **2025**. [CrossRef]
44. Wurtz, R.H. Corollary Discharge Contributions to Perceptual Continuity across Saccades. *Annu. Rev. Vis. Sci.* **2018**, *15*, 4. [CrossRef] [PubMed]
45. Boubenec, Y.; Shulz, D.E.; Debrégeas, G. Whisker Encoding of Mechanical Events during Active Tactile Exploration. *Front. Behav. Neurosci.* **2012**, *6*, 74. [CrossRef]
46. Deutsch, D.; Pietr, M.; Knutsen, P.M.; Ahissar, E.; Schneidman, E. Fast Feedback in Active Sensing: Touch-Induced Changes to Whisker-Object Interaction. *PLoS ONE* **2012**, *7*, e44272. [CrossRef] [PubMed]
47. Szwed, M.; Bagdasarian, K.; Ahissar, E. Encoding of Vibrissal Active Touch. *Neuron* **2003**, *40*, 621–630. [CrossRef] [PubMed]
48. Gao, P.; Bermejo, R.; Zeigler, H.P. Whisker Deafferentation and Rodent Whisking Patterns: Behavioral Evidence for a Central Pattern Generator. *J. Neurosci. Off. J. Soc. Neurosci.* **2001**, *21*, 5374–5380. [CrossRef] [PubMed]
49. Carvell, G.E.; Simons, D.J. Biometric Analyses of Vibrissal Tactile Discrimination in the Rat. *J. Neurosci.* **1990**, *10*, 2638–2648. [CrossRef] [PubMed]
50. Hyde, J.E. Some Characteristics of Voluntary Human Ocular Movements in the Horizontal Plane. *Am. J. Ophthalmol.* **1959**, *48*, 85–94. [CrossRef] [PubMed]
51. Gugig, E.; Sharma, H.; Azouz, R. Gradient of Tactile Properties in the Rat Whisker Pad. *PLoS Biol.* **2020**, *18*, e3000699. [CrossRef] [PubMed]
52. Lottem, E.; Azouz, R. Mechanisms of Tactile Information Transmission through Whisker Vibrations. *J. Neurosci. Off. J. Soc. Neurosci.* **2009**, *29*, 11686–11697. [CrossRef] [PubMed]
53. Ko, H.-K.; Snodderly, D.M.; Poletti, M. Eye Movements between Saccades: Measuring Ocular Drift and Tremor. *Vision. Res.* **2016**, *122*, 93–104. [CrossRef] [PubMed]
54. McCamy, M.B.; Otero-Millan, J.; Leigh, R.J.; King, S.A.; Schneider, R.M.; Macknik, S.L.; Martinez-Conde, S. Simultaneous Recordings of Human Microsaccades and Drifts with a Contemporary Video Eye Tracker and the Search Coil Technique. *PLoS ONE* **2015**, *10*, e0128428. [CrossRef] [PubMed]
55. Aytekin, M.; Victor, J.D.; Rucci, M. The Visual Input to the Retina during Natural Head-Free Fixation. *J. Neurosci.* **2014**, *34*, 12701–12715. [CrossRef] [PubMed]
56. Haidarliu, S.; Bagdasarian, K.; Shinde, N.; Ahissar, E. Muscular Basis of Whisker Torsion in Mice and Rats. *Anat. Rec.* **2017**, *300*, 1643–1653. [CrossRef] [PubMed]
57. Ong, J.K.; Haslwanter, T. Measuring Torsional Eye Movements by Tracking Stable Iris Features. *J. Neurosci. Methods* **2010**, *192*, 261–267. [CrossRef] [PubMed]
58. Yarbus, A.L. *Eye Movements and Vision*; Plenum Press: New York, USA, 1967.
59. Hopf, S.; Liesenfeld, M.; Schmidtmann, I.; Ashayer, S.; Pitz, S. Age Dependent Normative Data of Vertical and Horizontal Reflexive Saccades. *PLoS ONE* **2018**, *13*, e0204008. [CrossRef] [PubMed]
60. Carpenter, R.H.S. *Movements of the Eyes*; Pion: London, UK, 1988.
61. Daye, P.M.; Optican, L.M.; Roze, E.; Gaymard, B.; Pouget, P. Neuromimetic Model of Saccades for Localizing Deficits in an Atypical Eye-Movement Pathology. *J. Transl. Med.* **2013**, *11*, 125. [CrossRef] [PubMed]
62. Baloh, R.W.; Sills, A.W.; Kumley, W.E.; Honrubia, V. Quantitative Measurement of Saccade Amplitude, Duration, and Velocity. *Neurology* **1975**, *25*, 1065–1070. [CrossRef] [PubMed]
63. Becker, W. The Neurobiology of Saccadic Eye Movements. *Metrics. Rev. Oculomot. Res.* **1989**, *3*, 13–67. [PubMed]
64. Bahill, A.T.; Brockenbrough, A.; Troost, B.T. Variability and Development of a Normative Data Base for Saccadic Eye Movements. *Investig. Ophthalmol. Vis. Sci.* **1981**, *21*, 116–125. [PubMed]
65. Donders, F.C.; Doijer, D. The Location of the Pivot Point of the Eye. Part II. *Strabismus* **2016**, *24*, 184–188. [CrossRef] [PubMed]
66. Haidarliu, S.; Golomb, D.; Kleinfeld, D.; Ahissar, E. Dorsorostral Snout Muscles in the Rat Subserve Coordinated Movement for Whisking and Sniffing. *Anat. Rec.* **2012**, *295*, 1181–1191. [CrossRef] [PubMed]
67. Silverman, R.T.; Munger, B.L.; Halata, Z. The Sensory Innervation of the Rat Rhinarium. *Anat. Rec.* **1986**, *214*, 210–225. [CrossRef] [PubMed]

68. Pardiñas, U.F.J.; Brito, J.; Soto, E.C.; Cañón, C. Comparative Morphology of the Rhinarium and Upper Lip in Sigmodontine Rodents: Refined Nomenclature, Intertribal Variation in a Phylogenetic Framework, and Functional Inferences. *J. Morphol.* **2024**, *285*, e21760. [CrossRef] [PubMed]
69. Rucci, M.; Ahissar, E.; Burr, D. Temporal Coding of Visual Space. *Trends Cogn. Sci.* **2018**, *22*, 883–895. [CrossRef] [PubMed]
70. Pammer, L.; O'Connor, D.H.; Hires, S.A.; Clack, N.G.; Huber, D.; Myers, E.W.; Svoboda, K. The Mechanical Variables Underlying Object Localization along the Axis of the Whisker. *J. Neurosci. Off. J. Soc. Neurosci.* **2013**, *33*, 6726–6741. [CrossRef] [PubMed]
71. Bagdasarian, K.; Szwed, M.; Knutsen, P.M.; Deutsch, D.; Derdikman, D.; Pietr, M.; Simony, E.; Ahissar, E. Pre-Neuronal Morphological Processing of Object Location by Individual Whiskers. *Nat. Neurosci.* **2013**, *16*, 622–631. [CrossRef] [PubMed]
72. Oladazimi, M.; Putelat, T.; Szalai, R. Conveyance of Texture Signals along a Rat Whisker. *Sci. Rep.* **2021**, *11*, 13570. Erratum in *Sci. Rep.* **2021**, *11*, 24233. https://doi.org/10.1038/s41598-021-03545-9. [CrossRef] [PubMed]
73. Quist, B.W.; Hartmann, M.J.Z. Mechanical Signals at the Base of a Rat Vibrissa: The Effect of Intrinsic Vibrissa Curvature and Implications for Tactile Exploration. *J. Neurophysiol.* **2012**, *107*, 2298–2312. [CrossRef] [PubMed]
74. Hartmann, M.J.; Johnson, N.J.; Towal, R.B.; Assad, C. Mechanical Characteristics of Rat Vibrissae: Resonant Frequencies and Damping in Isolated Whiskers and in the Awake Behaving Animal. *J. Neurosci.* **2003**, *23*, 6510–6519. [CrossRef] [PubMed]
75. Szwed, M.; Bagdasarian, K.; Blumenfeld, B.; Barak, O.; Derdikman, D.; Ahissar, E. Responses of Trigeminal Ganglion Neurons to the Radial Distance of Contact during Active Vibrissal Touch. *J. Neurophysiol.* **2006**, *95*, 791–802. [CrossRef] [PubMed]
76. Knutsen, P.M.; Ahissar, E. Orthogonal Coding of Object Location. *Trends Neurosci.* **2009**, *32*, 101–109. Erratum in *Trends Neurosci.* **2009**, *32*, 187–188. https://doi.org/10.1016/j.tins.2009.02.001. [CrossRef] [PubMed]
77. Neimark, M.A.; Andermann, M.L.; Hopfield, J.J.; Moore, C.I. Vibrissa Resonance as a Transduction Mechanism for Tactile Encoding. *J. Neurosci.* **2003**, *23*, 6499–6509. [CrossRef] [PubMed]
78. Andermann, M.L.; Ritt, J.; Neimark, M.A.; Moore, C.I. Neural Correlates of Vibrissa Resonance; Band-Pass and Somatotopic Representation of High-Frequency Stimuli. *Neuron* **2004**, *42*, 451–463. [CrossRef] [PubMed]
79. Arabzadeh, E.; Zorzin, E.; Diamond, M.E. Neuronal Encoding of Texture in the Whisker Sensory Pathway. *PLoS Biol.* **2005**, *3*, e17. [CrossRef] [PubMed]
80. Wolfe, J.; Hill, D.N.; Pahlavan, S.; Drew, P.J.; Kleinfeld, D.; Feldman, D.E. Texture Coding in the Rat Whisker System: Slip-Stick versus Differential Resonance. *PLoS Biol.* **2008**, *6*, e215. [CrossRef] [PubMed]
81. Oladazimi, M.; Brendel, W.; Schwarz, C. Biomechanical Texture Coding in Rat Whiskers. *Sci. Rep.* **2018**, *8*, 11139. [CrossRef] [PubMed]
82. Ebara, S.; Kumamoto, K.; Matsuura, T.; Mazurkiewicz, J.E.; Rice, F.L. Similarities and Differences in the Innervation of Mystacial Vibrissal Follicle-Sinus Complexes in the Rat and Cat: A Confocal Microscopic Study. *J. Comp. Neurol.* **2002**, *449*, 103–119. [CrossRef] [PubMed]
83. Rice, F.L.; Mance, A.; Munger, B.L. A Comparative Light Microscopic Analysis of the Sensory Innervation of the Mystacial Pad. I. Innervation of Vibrissal Follicle-Sinus Complexes. *J. Comp. Neurol.* **1986**, *252*, 154–174. [CrossRef] [PubMed]
84. Tonomura, S.; Ebara, S.; Bagdasarian, K. Structure-Function Correlations of Rat Trigeminal Primary Neurons: Emphasis on Club-like Endings, a Vibrissal Mechanoreceptor. *Proc. Jpn. Acad. Ser. B Phys. Biol. Sci.* **2015**, *91*, 560–576. Erratum in *Proc. Jpn. Acad. Ser. B Phys. Biol. Sci.* **2016**, *92*, 76. [CrossRef] [PubMed]
85. Handler, A.; Ginty, D.D. The Mechanosensory Neurons of Touch and Their Mechanisms of Activation. *Nat. Rev. Neurosci.* **2021**, *22*, 521–537. [CrossRef] [PubMed]
86. Ranade, S.S.; Woo, S.-H.; Dubin, A.E. Piezo2 Is the Major Transducer of Mechanical Forces for Touch Sensation in Mice. *Nature* **2014**, *516*, 121–125. [CrossRef] [PubMed]
87. Ebara, S.; Furuta, T.; Kumamoto, K. Vibrissal Mechanoreceptors. *Scholarpedia* **2017**, *12*, 32372. [CrossRef]
88. Poole, K.; Herget, R.; Lapatsina, L.; Ngo, H.-D.; Lewin, G.R. Tuning Piezo Ion Channels to Detect Molecular-Scale Movements Relevant for Fine Touch. *Nat. Commun.* **2014**, *5*, 3520. [CrossRef] [PubMed]
89. Evans, M.H.; Loft, M.S.E.; Campagner, D.; Petersen, R.S. Sensing the Environment With Whiskers. In *Oxford Research Encyclopedia of Neuroscience*; Sherman, S.M., Ed.; Oxford University Press: Oxford, UK, 2019.
90. Woo, S.-H.; Ranade, S.; Weyer, A.D. Piezo2 Is Required for Merkel-Cell Mechanotransduction. *Nature* **2014**, *509*, 622–626. [CrossRef] [PubMed]
91. Pitts, D.S.; Cullen, A.P.; Hacker, P.D. Ocular Effects of Ultraviolet Radiation from 295 to 365 nm. *Investig. Ophthalmol. Vis. Sci.* **1977**, *16*, 932–939. [PubMed]
92. Sliney, D.H. How Light Reaches the Eye and Its Components. *Int. J. Toxicol.* **2002**, *21*, 501–509. [CrossRef] [PubMed]
93. Palczewski, P. Chemistry and Biology of the Initial Steps in Vision: The Friedenwald Lecture. *Investig. Ophthalmol. Vis. Sci.* **2014**, *55*, 6651–6672. [CrossRef] [PubMed]
94. Hosoya, T.; Baccus, S.A.; Meister, M. Dynamic Predictive Coding by the Retina. *Nature* **2005**, *436*, 71–77. [CrossRef] [PubMed]
95. Doly, M. Transduction of the Light Message: From the Photon to the Optic Nerve. *Fundam. Clin. Pharmacol.* **1994**, *8*, 147–154. [CrossRef] [PubMed]

96. Ayoub, G. A Window to the Brain—The Enduring Impact of Vision Research. *Brain Sci.* **2025**, *15*, 453. [CrossRef] [PubMed]
97. Schneider, K.A.; Kastner, S. Visual Responses of the Human Superior Colliculus: A High-Resolution Functional Magnetic Resonance Imaging Study. *J. Neurophysiol.* **2005**, *94*, 2491–2503. [CrossRef] [PubMed]
98. Belford, G.R.; Killackey, H.P. Vibrissae Representation in Subcortical Trigeminal Centers of the Neonatal Rat. *J. Comp. Neurol.* **1979**, *183*, 305–321. [CrossRef] [PubMed]
99. Gerhardt, B.; Alfken, J.; Reichmann, J.; Salditt, T.; Brecht, M. Three-Dimensional Architecture and Linearized Mapping of Vibrissa Follicle Afferents. *Nat. Commun.* **2025**, *16*, 499. [CrossRef] [PubMed]
100. Solomon, S.G.; Lennie, P. The Machinery of Colour Vision. *Nat. Rev. Neurosci.* **2007**, *8*, 276–286. [CrossRef] [PubMed]
101. Schiller, P.H. The ON and OFF Channels of the Visual System. *Trends Neurosci.* **1992**, *15*, 86–92. [CrossRef] [PubMed]
102. Yu, C.; Derdikman, D.; Haidarliu, S.; Ahissar, E. Parallel Thalamic Pathways for Whisking and Touch Signals in the Rat. *PLoS Biol.* **2006**, *4*, e124. [CrossRef] [PubMed]
103. Veinante, P.; Jacquin, M.F.; Deschênes, M. Thalamic Projections from the Whisker-Sensitive Regions of the Spinal Trigeminal Complex in the Rat. *J. Comp. Neurol.* **2000**, *420*, 233–243. [CrossRef]
104. Bloomfield, S.A.; Xin, D. Surround Inhibition of Mammalian AII Amacrine Cells Is Generated in the Proximal Retina. *J. Physiol.* **2000**, *523*, 771–783. [CrossRef] [PubMed]
105. Lo, F.S.; Guido, W.; Erzurumlu, R.S. Electrophysiological Properties and Synaptic Responses of Cells in the Trigeminal Principal Sensory Nucleus of Postnatal Rats. *J. Neurophysiol.* **1999**, *82*, 2765–2775. [CrossRef] [PubMed]
106. Hobbs, J.A.; Towal, R.B.; Hartmann, M.J.Z. Spatiotemporal Patterns of Contact Across the Rat Vibrissal Array During Exploratory Behavior. *Front. Behav. Neurosci.* **2016**, *9*, 356. [CrossRef] [PubMed]
107. Ahissar, E.; Knutsen, P.M. Object Localization with Whiskers. *Biol. Cybern.* **2008**, *98*, 449–458. [CrossRef] [PubMed]
108. Nogueira, R.; Rodgers, C.C.; Bruno, R.M.; Fusi, S. The Geometry of Cortical Representations of Touch in Rodents. *Nat. Neurosci.* **2023**, *26*, 239–250. [CrossRef] [PubMed]
109. Gollisch, T.; Meister, M. Rapid Neural Coding in the Retina with Relative Spike Latencies. *Science* **2008**, *319*, 1108–1111. [CrossRef] [PubMed]
110. Hires, S.A.; Gutnisky, D.A.; Yu, J.; O'Connor, D.H.; Svoboda, K. Low-Noise Encoding of Active Touch by Layer 4 in the Somatosensory Cortex. *eLife* **2015**, *4*, e06619. [CrossRef] [PubMed]
111. Petersen, R.S.; Panzeri, S.; Diamond, M.E. Population Coding of Stimulus Location in Rat Somatosensory Cortex. *Neuron* **2001**, *32*, 503–514. [CrossRef] [PubMed]
112. Srinath, R.; Ni, A.M.; Marucci, C.; Cohen, M.R.; Brainard, D.H. Orthogonal Neural Representations Support Perceptual Judgments of Natural Stimuli. *Sci. Rep.* **2025**, *15*, 5316. [CrossRef] [PubMed]
113. Benucci, A.; Ringach, D.L.; Carandini, M. Coding of Stimulus Sequences by Population Responses in Visual Cortex. *Nat. Neurosci.* **2009**, *12*, 1317–1324. [CrossRef] [PubMed]
114. Rucci, M.; Victor, J.D. The Unsteady Eye: An Information-Processing Stage, Not a Bug. *Trends Neurosci.* **2015**, *38*, 195–206. [CrossRef] [PubMed]
115. Ahissar, E.; Arieli, A. Seeing via Miniature Eye Movements: A Dynamic Hypothesis for Vision. *Front. Comput. Neurosci.* **2012**, *6*, 89. [CrossRef] [PubMed]
116. Assa, E.; Rivkind, A.; Kreiserman, M.; Khan, F.S.; Khan, S.; Ahissar, E. Temporal Coding Enables Hyperacuity in Event-Based Vision. *Nat. Commun.* **2026**, *17*, 9951. [CrossRef] [PubMed]
117. Ahissar, E.; Nelinger, G.; Assa, E.; Karp, O.; Saraf-Sinik, I. Thalamocortical Loops as Temporal Demodulators across Senses. *Commun. Biol.* **2023**, *6*, 562. [CrossRef] [PubMed]
118. Dacey, D.M.; Packer, O.S. Colour Coding in the Primate Retina: Diverse Cell Types and Cone-Specific Circuitry. *Curr. Opin. Neurobiol.* **2003**, *13*, 421–427. [CrossRef] [PubMed]
119. Wandell, B.A.; Dumoulin, S.O.; Brewer, A.A. Visual Field Maps in Human Cortex. *Neuron* **2007**, *56*, 366–383. [CrossRef] [PubMed]
120. Reich, D.S.; Mechler, F.; Victor, J.D. Temporal Coding of Contrast in Primary Visual Cortex: When, What, and Why. *J. Neurophysiol.* **2001**, *85*, 1039–1050. [CrossRef] [PubMed]
121. Kuruppath, P.; Gugig, E.; Azouz, R. Microvibrissae-Based Texture Discrimination. *J. Neurosci.* **2014**, *34*, 5115–5120. [CrossRef] [PubMed]
122. Hubel, D.H.; Wiesel, T.N. Receptive Fields and Functional Architecture of Monkey Striate Cortex. *J. Physiol.* **1968**, *195*, 215–243. [CrossRef] [PubMed]
123. De Valois, R.L.; William Yund, E.; Hepler, N. The Orientation and Direction Selectivity of Cells in Macaque Visual Cortex. *Vision. Res.* **1982**, *22*, 531–544. [CrossRef] [PubMed]
124. De Valois, R.L.; Albrecht, D.G.; Thorell, L.G. Spatial Frequency Selectivity of Cells in Macaque Visual Cortex. *Vision. Res.* **1982**, *22*, 545–559. [CrossRef] [PubMed]
125. Albright, T.D. Direction and Orientation Selectivity of Neurons in Visual Area MT of the Macaque. *J. Neurophysiol.* **1984**, *52*, 1106–1130. [CrossRef] [PubMed]

126. Petersen, R.S.; Diamond, M.E. Spatial–Temporal Distribution of Whisker-Evoked Activity in Rat Somatosensory Cortex and the Coding of Stimulus Location. *J. Neurosci.* **2000**, *20*, 6135–6143. [CrossRef] [PubMed]
127. Estebanez, L.; Boustani, S.E.; Destexhe, A.; Shulz, D.E. Correlated Input Reveals Coexisting Coding Schemes in a Sensory Cortex. *Nat. Neurosci.* **2012**, *15*, 1691–1699. [CrossRef] [PubMed]
128. Rodgers, C.C.; Nogueira, R.; Pil, B.C.; Greeman, E.A.; Park, J.M.; Hong, Y.K.; Fusi, S.; Bruno, R.M. Sensorimotor Strategies and Neuronal Representations for Shape Discrimination. *Neuron* **2021**, *109*, 2308–2325.e10. [CrossRef] [PubMed]
129. Dumoulin, S.O.; Wandell, B.A. Population Receptive Field Estimates in Human Visual Cortex. *NeuroImage* **2008**, *39*, 647–660. [CrossRef] [PubMed]
130. Wang, X.; Zhang, S.-H.; Tang, S.-M.; Yu, C. Orthogonal Neural Geometry of Orientation, Spatial Frequency, and Ocular Dominance in Macaque V1. *Prog. Neurobiol.* **2026**, *258*, 102874. [CrossRef] [PubMed]
131. Land, M.F.; Nilsson, D.-E. *Animal Eyes (Oxford Animal Biology Series)*; Oxford University Press: Oxford, UK, 2012. [CrossRef]
132. Ahissar, E.; Assa, E. Perception as a Closed-Loop Convergence Process. *eLife* **2016**, *5*, e12830. [CrossRef] [PubMed]
133. Pearson, M.J.; Pipe, A.G.; Melhuish, C.; Mitchinson, B.; Prescott, T.J. Whiskerbot: A Robotic Active Touch System Modeled on the Rat Whisker Sensory System. *Adapt. Behav.* **2007**, *15*, 223–240. [CrossRef]
134. Pearson, M.J.; Mitchinson, B.; Welsby, J.; Pipe, T.; Prescott, T.J. SCRATCHbot: Active Tactile Sensing in a Whiskered Mobile Robot. In *From Animals to Animats 11*; Doncieux, S., Girard, B., Guillot, A., Hallam, J., Meyer, J.-A., Mouret, J.-B., Eds.; Springer: Berlin, Heidelberg, 2010; pp. 93–103. [CrossRef]
135. Van Opstal, A.J.; Alitappeh, R.J.; John, A.; Bernardino, A. Realistic 3D Human Saccades Generated by a 6-DOF Biomimetic Robotic Eye under Optimal Control. *Front. Robot. AI* **2024**, *11*, 1393637. [CrossRef] [PubMed]

Disclaimer/Publisher's Note: The statements, opinions and data contained in all publications are solely those of the individual author(s) and contributor(s) and not of MDPI and/or the editor(s). MDPI and/or the editor(s) disclaim responsibility for any injury to people or property resulting from any ideas, methods, instructions or products referred to in the content.